Classification of primary hepatic tumours in the dog

Van Sprundel, R G H M ; Van den Ingh, T S G A M ; Guscetti, Franco ; Kershaw, O ; Kanemoto, H ; van Gils, H M ; Rothuizen, J ; Roskams, T ; Spee, B

Abstract: Many advances have been made in the characterisation of primary liver tumours in humans, in particular relating to the identification and role of hepatic progenitor cells, resulting in a new classification. The aim of the present study was to investigate the presence and relative frequency of morphological types of canine primary hepatic neoplasms and to determine whether a classification similar to the human scheme can be applied to these canine neoplasms. Canine primary liver tumours (n=106) were examined histologically and with the immunohistochemical markers keratin 19, HepPar-1, epithelial membrane antigen/mucin-1, CD10, neuron-specific enolase and chromogranin-A. Eleven nodular hyperplasias and 82 tumours of hepatocellular origin were diagnosed. The latter were subdivided in hepatocellular tumours with 0-5% positivity for K19 (n=62), which were well differentiated and had no evidence of metastasis, tumours with >5% positivity for K19 (n=17), which were poorly differentiated and had intrahepatic and/or distant metastasis, and a scirrhous subgroup (n=3) with an intermediate position with regard to K19 staining and malignancy. Ten cholangiocellular tumours (nine cholangiocellular carcinomas and one cholangiolocarcinoma) were diagnosed and all had intrahepatic and/or distant metastases. Three neuroendocrine carcinomas were also diagnosed. Histopathological and immunohistochemical examination of canine primary hepatic neoplasms can differentiate hepatocellular, cholangiocellular and neuroendocrine tumours, in accordance with the most recent human classification system.

DOI: https://doi.org/10.1016/j.tvjl.2013.05.027

Classification of primary hepatic tumours in the dog

Renee G.H.M. van Sprundel [a], Ted S.G.A.M. van den Ingh [b], Franco Guscetti [c], Olivia Kershaw [d], Hideyuki Kanemoto [e], Henrika M. van Gils [a], Jan Rothuizen [a], Tania Roskams [f], Bart Spee [a],

a Department of Clinical Sciences of Companion Animals, Faculty of Veterinary Medicine, Utrecht University, Utrecht, The Netherlands

b TCCI Consultancy BV, Utrecht, The Netherlands

c Institute of Veterinary Pathology, University of Zürich, Switzerland

d Institute of Veterinary Pathology, Free University Berlin, Germany

e Department of Veterinary Internal Medicine, Graduate School of Agricultural and Life Sciences, The University of Tokyo, Tokyo, Japan

f Department of Morphology and Molecular Pathology, University Hospitals Leuven, Leuven, Belgium

Abstract

Many advances have been made in the characterisation of primary liver tumours in humans, in particular relating to the identification and role of hepatic progenitor cells, resulting in a new classification. The aim of the present study was to investigate the presence and relative frequency of morphological types of canine primary hepatic neoplasms and to determine whether a classification similar to the human scheme can be applied to these canine neoplasms. Canine primary liver tumours (n = 106) were examined histologically and with the immunohistochemical markers keratin 19, HepPar-1, epithelial membrane antigen/mucin-1, CD10, neuron-specific enolase and chromogranin-A. Eleven nodular hyperplasias and 82 tumours of hepatocellular origin were diagnosed. The latter were subdivided in hepatocellular tumours with 0–5% positivity for K19 (n = 62), which were well differentiated and had no evidence of metastasis, tumours with >5% positivity for K19 (n = 17), which were poorly differentiated and had intra- hepatic and/or distant metastasis, and a scirrhous subgroup (n = 3) with an intermediate position with regard to K19 staining and malignancy. Ten cholangiocellular tumours (nine cholangiocellular carcinomas and one cholangiolocarcinoma) were diagnosed and all had intrahepatic and/or distant metastases. Three neuroendocrine carcinomas were also diagnosed. Histopathological and immunohistochemical examination of canine primary hepatic neoplasms can differentiate hepatocellular, cholangiocellular and neuroendocrine tumours, in accordance with the most recent human classification system.

Introduction

Primary liver tumours in dogs are relatively rare, representing 0.6–1.5% of all tumours in dogs (Patnaik et al., 1980, 1981). No predisposing factors are known and, in almost all cases, no additional primary liver pathology is present (Hammer and Sikkema, 1995; Watson, 2005). Currently, canine neoplasms are classified as hepatocellular adenomas and carcinomas, cholangiocellular adenomas and carcinomas, mixed hepatocellular and cholangiocellular carcinomas, and hepatic carcinoids (Cullen and Popp, 2002; Charles et al., 2006; Stalker and Hayes, 2007); to date, hepatoblastomas have not been recognised in the dog (Charles et al., 2006).

Over the past decade, many advances have been made in the characterisation of primary liver tumours in humans, in particular relating to the identification and significance of hepatic progenitor cells (HPCs) (Allison and Lovell, 2005; Libbrecht, 2006; Roskams, 2006). HPCs are multipotent cells, located within the canals of Hering, with the capacity for self-renewal and differentiation into mature hepatocytes and cholangiocytes (Libbrecht and Roskams, 2002; Turner et al., 2011; Boulter et al., 2012). In primary hepatocellular tumours of dogs, tumours with HPC characteristics are poorly differentiated and aggressive (van Sprundel et al., 2010). Recent studies of the role of HPCs in the development and differentiation of intrahepatic cholangiocellular tumours in humans have resulted in a new histomorphological and immunohistochemical classification of primary liver tumours in humans, taking into account their aggressiveness and prognosis (Komuta et al., 2008, 2012).

In humans, primary liver tumours may arise from mature hepatocytes or cholangiocytes, representing hepatocellular and cholangiocellular adenomas and carcinomas, respectively (Fig. 1). Hepatic tumours may also arise from HPCs; such neoplasms exhibit varying degrees of differentiation, sometimes with overlapping morphological features, e.g. cholangiolocarcinomas (Komuta et al., 2008, 2012; Yeh, 2010). Cholangiolocarcinomas are thought to originate from the canals of Hering and have hepatocellular, ductular and cholangiocellular characteristics (Komuta et al., 2008, 2012; Seok et al., 2012).

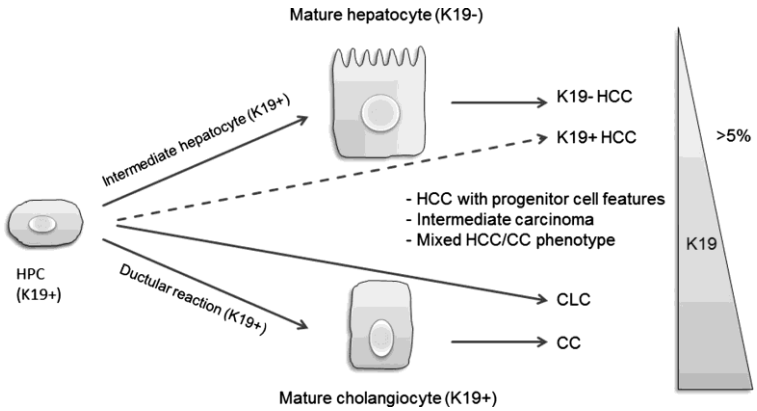

Fig. 1. Proposed origin and classification of primary liver tumours in humans. Primary liver tumours may arise from mature hepatocytes or cholangiocytes, representing the classic hepatocellular and cholangiocellular adenomas and carcinomas. They may also arise from hepatic progenitor cells showing varying degrees of differentiation and develop various and sometimes overlapping morphological features, such as cholangiolocarcinomas. HPC, hepatic progenitor cell; HCC, hepatocellular carcinoma; CC, cholangiocellular carcinoma; CLC, cholangiolocarcinoma; K19, keratin 19.

Primary hepatic neoplasms in dogs can be classified and differentiated using immunohistochemical stains for markers representative of hepatocytic and cholangiocytic lineages (Lau et al., 2002; Morrison et al., 2002; Libbrecht, 2006; van Sprundel et al., 2010; Al-Muhannadi et al., 2011). The aim of the present study was to investigate the occurrence and relative frequency of various morphological types of primary hepatic neoplasms in the dog and to determine whether a classification similar to the human scheme can be applied to canine hepatic neoplasms.

Materials and methods

Samples

Formalin-fixed paraffin-embedded material from primary liver tumours of 106 dogs was available from the archives of the Department of Pathobiology, Utrecht University (n = 18), Valuepath, Laboratory for Veterinary Pathology, Hoensbroek, The Netherlands (n = 28), the Institute of Veterinary Pathology, University of Zürich, Switzerland (n = 46), and the Institute of Veterinary Pathology, Free University Berlin, Germany (n = 14). All material was derived from clinical cases and had been submitted for individual diagnostic purposes; no tissue was collected specifically for the purpose of the present study. Formalin-fixed paraffin-embedded samples from the livers of healthy dogs, as well as a sample from a dog with fulminant hepatitis and reactive ductular proliferation, were available from the Department of Clinical Sciences of Companion Animals, Utrecht University.

Grading and staging

Histological grading and staging of the tumours was performed as described by van Sprundel et al. (2010). The parameters scored from 0 to 3 for grading comprised cell and nuclear pleomorphism, presence or absence of multinucleated tumour cells and mitotic activity. Three stages were based on histopathology, anamnestic data (ultrasonography and surgery reports, including follow-up data from referring veterinarians and/or owners) and postmortem pathology reports: (1) stage 0: Macroscopically only one tumour process was present in the liver and/or microscopically the tumour was well circumscribed or encapsulated; there was no evidence of intrahepatic and/or extrahepatic metastases; (2) stage 1: Microscopically the tumour had spread beyond the original (primary) site to the adjacent tissue, there was evidence of intravascular spread or the presence of microsatellites and/or multiple tumour processes were present in the liver macroscopically; and (3) stage 2: The tumour had spread from the primary site to the regional lymph nodes and/or other organs (distant metastasis).

Immunohistochemistry

Immunohistochemistry was performed for keratin 19 (K19), HepPar-1, epithelial membrane antigen/mucin-1 (EMA/MUC-1), CD10, neuron-specific enolase (NSE), and chromogranin-A (Cg-A) (Table 1). Negative controls were performed by replacing the primary antibody with washing buffer. Adrenal glands served as a positive control for NSE and Cg-A.

Results

Bile ducts in the liver from a healthy dog had strong cytoplasmic staining for K19 (Fig. 2A) and EMA/MUC-1 (Fig. 2D). There was moderate to marked cytoplasmic staining of hepatocytes for HepPar-1, probably depending on glycogen content (Fig. 2C). CD10 exhibited mild to marked canalicular staining and apical membranous staining of the smallest bile ducts (Fig. 2E); activated hepatic stellate cells exhibited positive immunostaining, whereas large bile ducts were negative (Fig. 2F). Strong positive staining for K19 was evident in reactive HPCs in areas of ductular proliferation in the canine liver with hepatitis (Fig. 2B), whereas these cells were negative for NSE and Cg-A. In the healthy liver, rare NSE positive epithelial cells were present in the epithelial lining of a larger bile duct; Cg-A was always negative.

Table 1

Antibody characteristics and experimental procedures for immunohistochemistry.

Antibody	Manufacture	Type	Clone	Antigen retrieval	Dilution	Wash buffer	Incubation
K 19	Novocastra	Mouse	B170	Proteinase K	1:100	TBS	1 h RT
HepPar-1	Dakocytomati	Mouse	OCH1E5	TBS/EDTA	1:50	PBS	Overnight 4 C
CD10	Novocastra	Mouse	56C6	Epitope retrieval solution 2	Ready to use	Bond wash solution 10x concentrate	0.5 h RT
EMA/MUC-1	Biosciences	Rabbit pAb	LS-C30532	TBS/EDTA	1:700	PBS	24 h 4 C
NSE	Dakocytomati	Mouse	BBS/NC/VI-H14	Citrate	1:400	PBS	Overnight 4 C
Cg-A	MP Products	Rabbit mAb	20086 SP-1	No antigen retrieval	1:800	PBS	Overnight 4 C

Cg-A, chromogranin-A; EDTA, ethylene diamine tetraacetic acid; EMA/MUC-1, epithelial membrane antigen/mucin-1; K19, keratin 19; mAb, monoclonal antibody; NSE, neuron-specific enolase; O/N, overnight; PBS, phosphate-buffered saline; pAb, polyclonal antibody; Prot K, proteinase K; RT, room temperature; TBS, Tris-buffered saline.

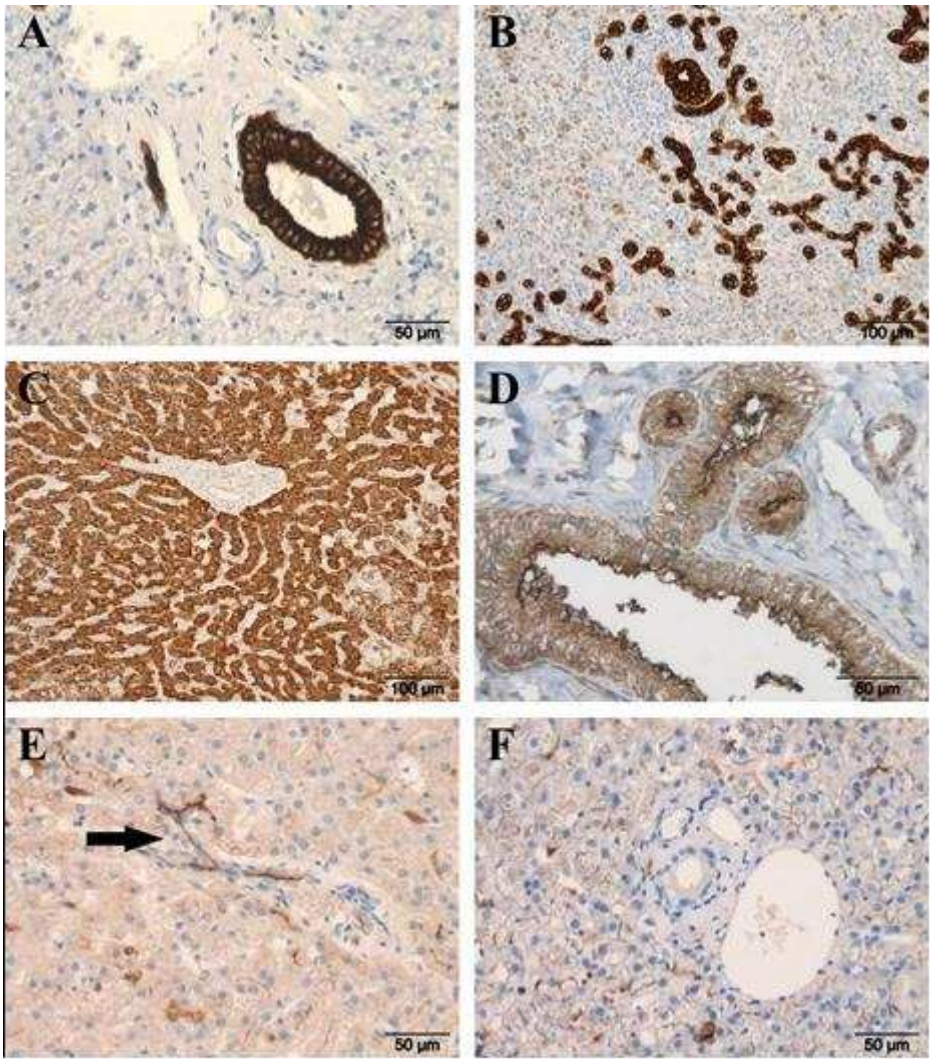

Fig. 2. Immunohistochemical staining of non-tumorous liver tissue. (A) K19, normal liver, portal area with positive staining bile duct and ductule; (B) K19, acute fulminant hepatitis with positive staining of reactive ductular proliferation; (C) HepPar-1, normal liver, marked staining of hepatic cords, portal area negative; (D) EMA/MUC-1, normal liver, positive staining bile duct; (E) CD10, normal liver, moderate positive staining of canaliculi, apical staining of smallest bile duct (arrow) and positive staining of hepatic stellate cells; (F) CD10, normal liver, marked canalicular staining, negative staining of larger bile ducts in portal area

On histopathological and immunohistochemical examination, the 106 primary liver tumours were classified as 11 nodular hyperplasias (10%), 82 hepatocellular tumours (77%), 10 cholangiocellular tumours (9%) and three hepatic neuroendocrine tumours (3%). There was no apparent sex or breed predisposition for a particular tumour type. The age of the dogs ranged from 6 to 18 years; younger dogs mostly were larger or giant breeds, but no statistical analysis was undertaken. In four dogs with cholangiocellular tumours, the livers also had fibrous areas with conglomerates of irregularly formed cystic / dilated bile ducts, consistent with adult-type congenital cystic liver disease (van den Ingh et al., 2006), whereas in the other dogs the non-neoplastic liver parenchyma was histologically normal.

Nodular hyperplasia (n = 11)

Histologically, hyperplastic nodules contained double layered cords of well-differentiated hepatocytes with slight compression of the surrounding parenchyma (Fig. 3A); characteristically, portal areas were present within the hyperplastic nodules (Fig. 3D). Hepatocytes had a uniform and normal appearance, and there

was no mitotic activity (grade 0). All hyperplastic nodules had moderate to marked cytoplasmic staining for HepPar-1 (Fig. 3B) and mild to marked canalicular staining for CD10 (Fig. 3C), but were negative for K19 (Fig. 3D), EMA/MUC-1, NSE and Cg-A.

Hepatocellular tumours (n = 82)

Hepatocellular tumours were divided in three groups on the basis of histopathological features and immunohistochemical staining for K19 (Table 2).

Hepatocellular tumours with 0–5% cells positive for K19 (n = 62)

Fifty-seven tumours of this type were received as surgical specimens and five were obtained at postmortem examination. On histopathological examination, these tumours were well demarcated and encapsulated, and consisted of broad trabeculae of well differentiated hepatocytes (Fig. 4A) separated by fine fibrovascular stroma and sometimes widely dilated sinusoids and cavernous blood-filled spaces; regularly, haemorrhagic and/or necrotic areas were present. In one case with medium-sized tumour cells, acinar configurations were present in addition to trabecular areas. The hepatocytes were well differentiated and had no or limited cellular pleomorphism, with no or rare mitotic figures (grade 0–2); they regularly showed areas with swollen glycogen-rich hepatocytes or hepatocellular steatosis and sometimes contained foci of extramedullary haematopoiesis. There was no evidence of infiltrative growth, intrahepatic vascular invasion or metastases. The tumours had moderate to marked positive cytoplasmic staining for HepPar-1 (Fig. 4B) and minimal to marked canalicular staining for CD10 (Fig. 4C). Staining for K19 was negative in most tumours (Fig. 4D); there were 1–5% positive tumour cells with cytoplasmic or membranous staining in 16/62 (25.8%) cases (Fig. 4E). EMA/ MUC-1 staining was negative in all tumours (Fig. 4F). Ten tumours were positive (<20% of cells) for NSE and one of these tumours was also positive for Cg-A (<5%).

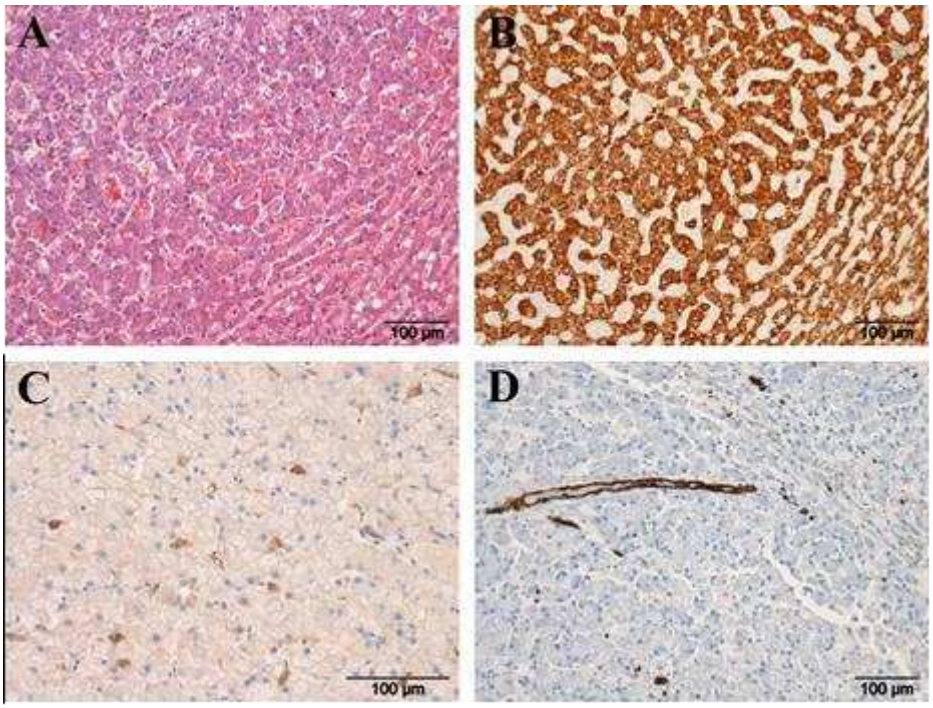

Fig. 3. Nodular hyperplasia. (A) HE, nodular hyperplasia with bilayered hepatic cords; compressed pre-existent liver tissue (lower right); (B) HepPar-1, positive staining of hepatocytes in both nodular hyperplasia and compressed pre-existent tissue (lower right); (C) CD10, mild canalicular staining and positive hepatic stellate cells; (D) K19, positive pre-existent bile duct within the negative staining nodular hyperplasia, compressed negative pre-existent parenchyma (upper right).

Table 2

Histological classification and immunohistochemistry of canine hepatocellular tumours.

	K19	Grading	Staging	HepPar-1	NSE	Cg-A	CD10	EMA/MUC-1
HCT 0–5% K19+	0% (n = 46)	0 (n = 10)	0 (n = 62)	100% (n = 54)	0% (n = 52)	0% (n = 61)	30–100%	0% (n = 62)
	1–5% (n = 16)	1 (n = 35)		60–90% (n = 8)	5–20% (n = 10)	5% (n = 1)	(n = 62)	
HCT >5% K19+	40–100% (n = 17)	1 (n = 3)	1 (n = 4)	0% (n = 15)	0% (n = 15)	0% (n = 16)	0% (n = 17)	0% (n = 17)
		2 (n = 6)	2 (n = 13)	5–20% (n = 2)	20–40% (n = 2)	5% (n = 1)		
sHCT	Ductular 100%	0 (n = 1)	0 (n = 2)	Ductular 0%	Ductular 100%	0% (n = 3)	Ductular 0%	0% (n = 3)
	Trabecular 0% Solid 100% (n = 3)	1 (n = 2)	1 (n = 1)	Trabecular 100% Solid 0% (n = 3)	Trabecular 0% Solid 80% (n = 3)		Trabecular 50% Solid 5% (n = 3)	

Cg-A, chromogranin-A; EMA/MUC-1, epithelial membrane antigen/mucin-1; HCT, hepatocellular tumour; K19, keratin 19; NSE, neuron-specific enolase; sHCT, scirrhous hepatocellular tumour.

Hepatocellular tumours with >5% cells positive for K19 (n = 17)

Twelve tumours of this type were obtained at postmortem examination and five were received as surgical specimens. Histologically, these tumours formed irregular trabeculae and markedly infiltrated the surrounding parenchyma. The cells were small compared to normal hepatocytes and were poorly differentiated, with marked cellular and nuclear pleomorphism, and many mitotic figures (up to 10 per high power field) (Fig. 5A). All exhibited lymphatic and vascular invasion in portal tracts (Fig. 5B) and had intrahepatic and/or distant metastases. The K19 positive cells in these tumours showed strong cytoplasmic staining (Fig. 5C). Most of the tumours were negative for HepPar-1 (Fig. 5D); in two cases, 5% and 20% of tumour cells were positive for this marker. CD10 (Fig. 5E) and EMA/MUC-1 were negative in all tumours. In two cases, 20% and 40% of the tumour cells were positive for NSE. In one case, 5% of tumour cells were positive for Cg-A.

Scirrhous hepatocellular tumours with K19 positive ductular structures (n = 3)

All of these tumours were received as surgical specimens. They contained areas with trabecular structures of well-differentiated hepatocytes (grade 0) and multifocal areas with a fibrous stromal component and ductular growth patterns (grade 1), whereby the trabecular areas were continuous with the ductular structures (Fig. 6A). The trabecular areas were strongly positive for HepPar-1 and moderately positive for CD10, but negative for K19 (Fig. 6B). The ductular structures in areas of fibrosis were positive for K19 (Fig. 6B) and NSE (Fig. 6C), but negative for HepPar-1 and CD10. The tumours were negative for EMA/MUC-1 and Cg-A. In two tumours, the ductular/fibrotic areas were well-circumscribed and were present within the well-differentiated trabecular component. In one tumour, the ductular component showed infiltrative growth, with ductular and solid areas in fibrous connective tissue adjacent to a large portal area (Fig. 6D). In this solid area, there was diffuse positivity for K19 (Fig. 6E) and irregular positivity for CD10 (Fig. 6F).

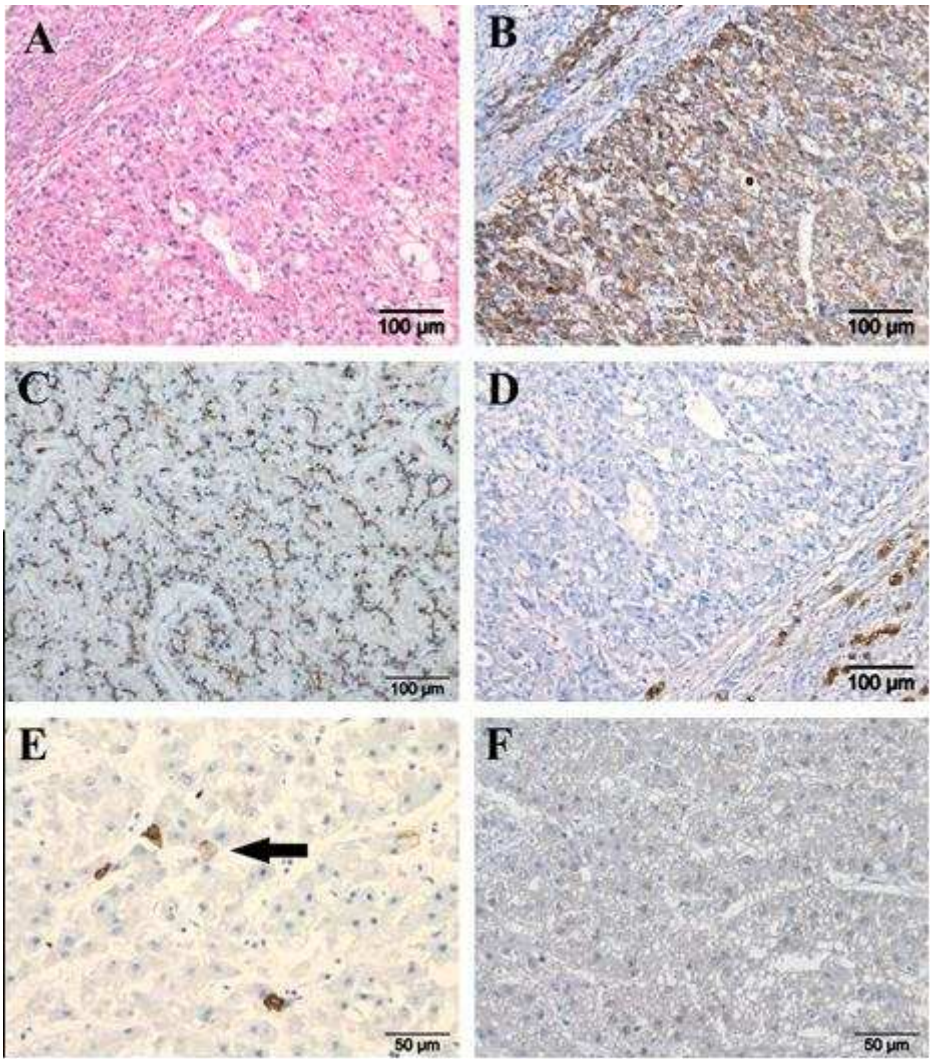

Fig. 4. Hepatocellular tumours 0–5% K19 positive. (A) HE, encapsulated tumour with moderate cellular pleiomorphism; (B) HepPar-1, marked cytoplasmic staining of neoplastic tissue; (C) CD10, marked canalicular staining in neoplastic tissue; (D) K19, neoplastic tissue negative, biliary proliferation in surrounding capsule positive; (E) K19, cells with either diffuse cytoplamic or membranous (arrow) staining in a less than 5% positive tumour; (F) EMA/MUC-1, negative staining of neoplastic tissue.

Cholangiocellular tumours (n = 10)

Ten tumours were classified as cholangiocellular carcinomas (9%) (Table 3). In most cases, cholangiocellular carcinomas were monomorphic, with an acinar, tubular and/or papillary growth pattern. In one case, the tumour had the characteristics of human cholangiolocarcinoma, with centrally located ductular structures, as well as more peripherally located solid areas with an hepatocellular appearance.

Cholangiocellular carcinomas (n = 9)

Two tumours were received as surgical specimens and seven were obtained at postmortem examination. These tumours had an acinar (Fig. 7A), tubular and/or papillary (Fig. 7B) growth pattern. The neoplastic cells were cuboidal to columnar, with a relatively small amount of cytoplasm, and had moderate to marked cellular and nuclear pleomorphism, with many mitotic figures (grade 2–3). All cholangiocellular tumours had vascular invasion and the presence of intrahepatic and/or distant metastases. Positive immunohistochemical staining for K19 was evident in 90–100% tumour cells in eight cases and 50–60% tumour cells in one case, with a cytoplasmic and, usually, more intense membranous staining (Fig. 7C). The tumours were also positive for EMA/MUC-1 (90–100% of tumour cells were immunopositive), with an apical membranous and/or diffuse cytoplasmic staining pattern (Figs. 7D and E), and were negative for HepPar-1 (Fig. 7F). Two of six tumours were negative for CD10 (Fig. 7G); in 4/6 cases, CD10 showed focal apical or cytoplasmic staining in tubulopapillary lesions within the tumour (Fig. 7H); there was insufficient tissue for CD10 immunostaining in three case. Two cases were positive for NSE (30% and 100% of tumour cells were immunopositive). Cg-A was negative in all cases.

Cholangiolocarcinoma (n = 1)

In one tumour, received as surgical specimen along with the corresponding regional lymph node, there was a combination of usually centrally located tubular structures, with or without fibrosis, and solid peripheral areas with a more hepatocellular appearance (Figs. 8A and B). The tumour showed moderate to marked cellular and nuclear pleomorphism, had a high mitotic activity (grade 3) and was classified as stage 2 because of vascular invasion and intra- hepatic and distant metastasis (Fig. 8C). Immunohistochemically, the tumour was negative for HepPar-1. K19 showed 90–100% positive staining, whereby the tubular areas showed diffuse cytoplasmic, as well as a more pronounced membranous, staining (Figs. 8D and E); the solid areas mainly showed moderate cytoplasmic staining for K19 (Fig. 8D). EMA/MUC-1 showed positive apical and/or cytoplasmic staining of tubular structures (Fig. 8F), whereas the solid structures were negative (Fig. 8G). CD10 was negative in the solid areas (Fig. 8H); apical and some cytoplasmic staining was present in the tubular areas (Fig. 8I) and moderate cytoplasmic staining was seen in intravascular metastases (Fig. 8J). There was focal cytoplasmic staining for Cg-A in the solid areas of the tumour. Immunostaining for NSE was negative.

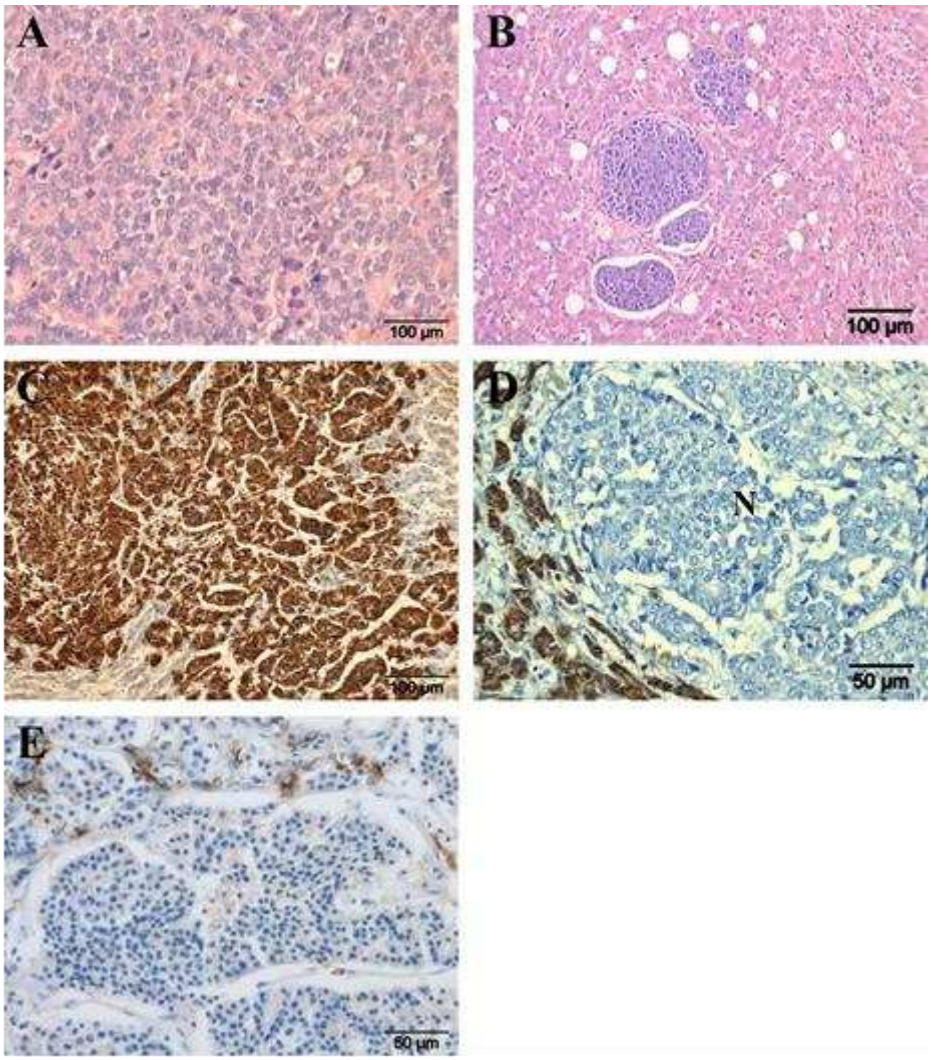

Fig. 5. Hepatocellular tumours with high K19 expression. (A) HE, relatively small tumour cells with abundant mitotic figures; (B) HE, vascular invasion and intrahepatic metastases; (C) K19, marked cytoplasmic staining of tumour cells; (D) HepPar-1, negative staining of neoplasm (N); (E) CD10, negative staining of neoplastic cells, some pre-existent hepatic cords with canalicular staining are present.

Neuroendocrine carcinomas (n = 3)

One tumour was received as a surgical specimen and two were obtained at postmortem examination. Histologically, neuroendocrine carcinomas consisted of medium-sized to large columnar cells with abundant cytoplasm and basal nuclei, and had a trabecular and/or rosette pattern of growth (Fig. 9A). The tumour cells showed only slight cellular and nuclear pleomorphism, the mitotic activity was moderate to high and the tumours were graded as 1. All tumours had evidence of intrahepatic metastases (stage 1). K19 staining was negative or <5% of the tumour cells were stained (Fig. 9B). HepPar-1 (Fig. 9C), CD10 and EMA/MUC-1 were negative in all cases. All the tumours showed >90% positivity for NSE (Fig. 9D). There was >30% immunopositivity for Cg-A in two of the tumours (Fig. 9E), whereas the third tumour was negative.

Discussion

In this study, 106 canine primary hepatic neoplasms were classified into morphologically well-defined groups on the basis of histopathological and immunohistochemical examination (Table 4). The classification system for dogs was based on recent systems for classifying hepatic tumours in humans (Komuta et al., 2008, 2012).

Nodular hyperplasia is a benign hepatocellular proliferation which occurs in many older dogs and can be found as single or multiple nodules, often as an incidental finding during laparotomy or at postmortem examination (Watson, 2005; Charles et al., 2006). The relatively low incidence of nodular hyperplasia (10%) in this study is likely to be related to the use of archival material, since hyperplastic nodules may not be submitted for histopathological evaluation as frequently as neoplasms.

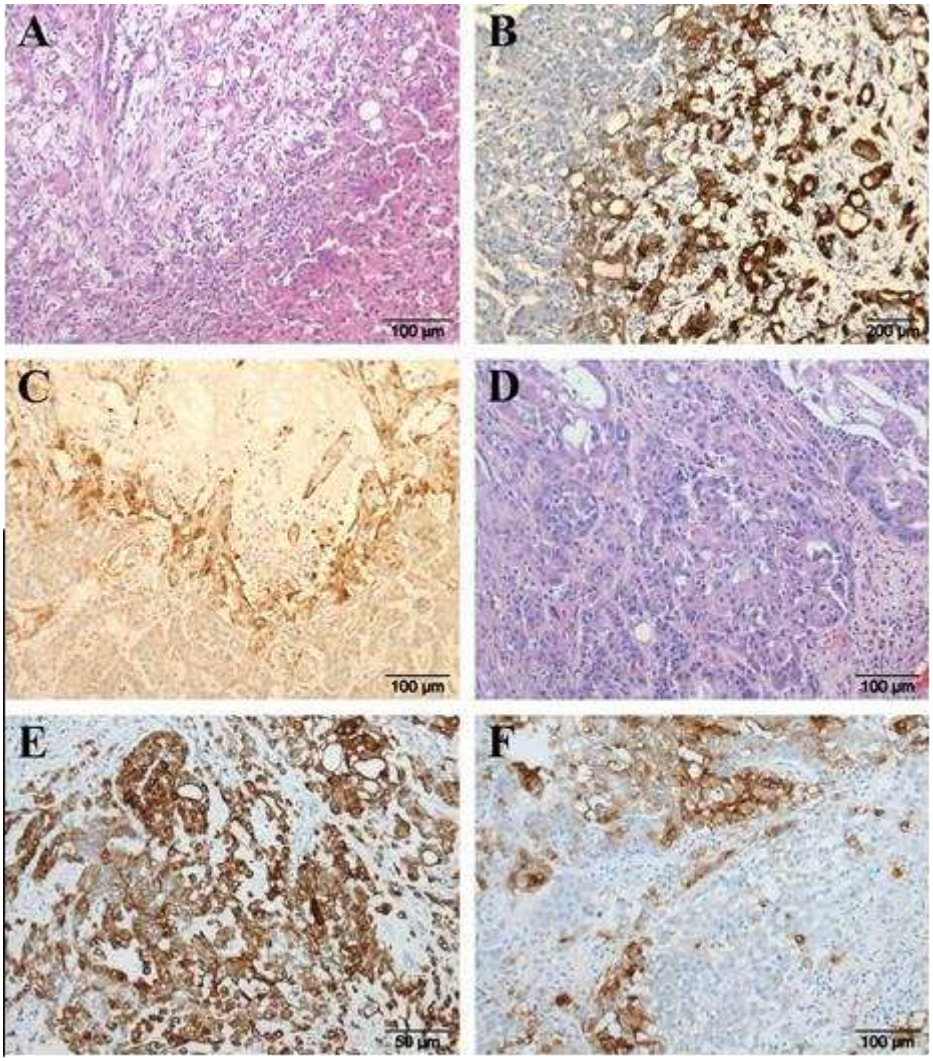

Fig. 6. Scirrhous hepatocellular tumours with K19 positive ductular structures. (A) HE, trabecular area with transition to ductular structures in fibrotic tissue; (B) K19, positive ductular structures continuous with negative trabecular area; (C) NSE, positive ductular structures continuous with negative trabecular area; (D) HE, solid area with malignant transformation and infiltrative growth; (E) K19, positive staining of solid malignant area; (F) CD10, local positive staining in malignant solid area.

Table 3

Histological classification and immunohistochemistry of the canine cholangiocellular tumours.

	K19	Grading	Staging	Hep Par-1	NSE	Cg-A	CD10	EMA/MUC-1
Cholangiocellular carcinoma	90–100% ($n = 8$) 50–60% ($n = 1$)	2 ($n = 5$) 3 ($n = 4$)	1 ($n = 3$) 2 ($n = 6$)	0% ($n = 9$)	0% ($n = 7$) 30–100% ($n = 2$)	0% ($n = 9$)	0% ($n = 2$) 20–30% ($n = 4$) NT ($n = 3$)	90–100% ($n = 6$) NT ($n = 3$)
Cholangiolocarcinoma	Tubular and solid 90–100% ($n = 1$)	3 ($n = 1$)	2 ($n = 1$)	0% ($n = 1$)	0% ($n = 1$)	Solid 5% ($n = 1$)	Tubular 100% Solid 0% ($n = 1$)	Tubular 100% Solid 0% ($n = 1$)

Cg-A, chromogranin-A; EMA/MUC-1, epithelial membrane antigen/mucin-1; K19, keratin 19; NSE, neuron-specific enolase; NT, not tested.

Hepatocellular tumours were the most common primary hepatic neoplasm in dogs in the present study. Nevertheless they appear to occur less frequently in dogs than in humans (Parkin et al., 2001), probably because a high proportion of human hepatocellular carcinomas arise from chronic infections with hepatitis B or hepatitis C viruses, both of which can lead to chronic inflammation and cirrhosis. In contrast, most canine hepatocellular tumours arise in otherwise normal appearing livers. As in humans, hepatocellular tumours in dogs could be divided into three subgroups, each with specific morphological and immunohistochemical characteristics. Canine tumours that were all or mostly K19 negative were most likely to be derived from mature hepatocytes and well circumscribed, with a low grade of cellular pleomorphism, and no evidence of infiltrative growth or metastases. However, a metastatic hepatocellular tumour (HepPar-1 positive; K19 status unknown) has recently been described in a dog (Lamoureux et al., 2012). In contrast, K19 positive canine tumours exhibited characteristics of HPCs without further differentiation towards cholangiocytic or hepatocellular lineages. These tumours may be derived from HPCs or through dedifferentiation of mature hepatocytes (Desmet, 2011). They had a high grade of cellular pleomorphism and exhibited infiltrative growth, vascular invasion and intrahepatic and/or extrahepatic metastases. This group comprised 21% of canine hepatocellular tumours; the frequency of this type of tumour in humans is 17% (Durnez et al., 2006).

The third and smallest group of hepatocellular tumours had an intermediate position with respect to histomorphology and immunohistochemistry. This group had the characteristics of well-differentiated hepatocellular tumours, but also showed multifocal stromal proliferation and formation of ductular structures; in 1/3 tumours, infiltrative growth suggested malignant transformation of the K19 positive structures. A similar morphological entity has been described in humans as scirrhous hepatocellular carcinoma, in which the stromal proliferation possibly drives K19 positive ductular differentiation (Wang et al., 2010).

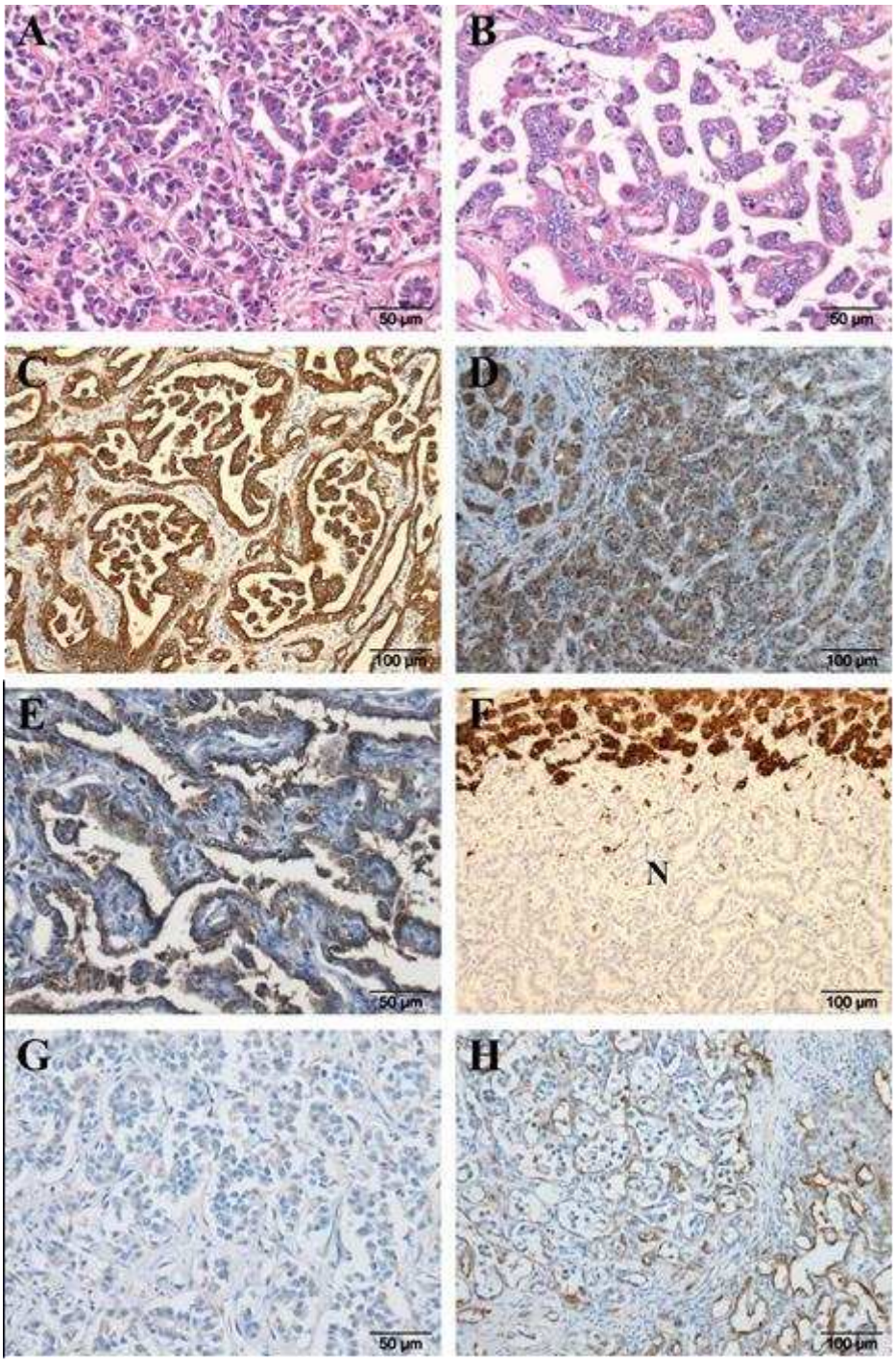

Fig. 7. Canine cholangiocellular carcinoma. (A) HE, acinar growth pattern; (B) HE, tubulopapillary growth pattern; (C) K19, marked positive staining of tubulopapillary area with cytoplasmic and membranous pattern; (D) EMA/MUC-1, diffuse cytoplasmic staining of neoplastic cells within acinar growth pattern; (E) EMA/MUC-1, positive cytoplasmic and apical staining of tumour cells in tubulopapillary growth pattern; (F) HepPar-1, negative staining of the tumour tissue (N); (G) CD10, negative staining of tumour cells within acinar growth pattern; (H) CD10, apical staining of tumour cells in tubulopapillary growth pattern.

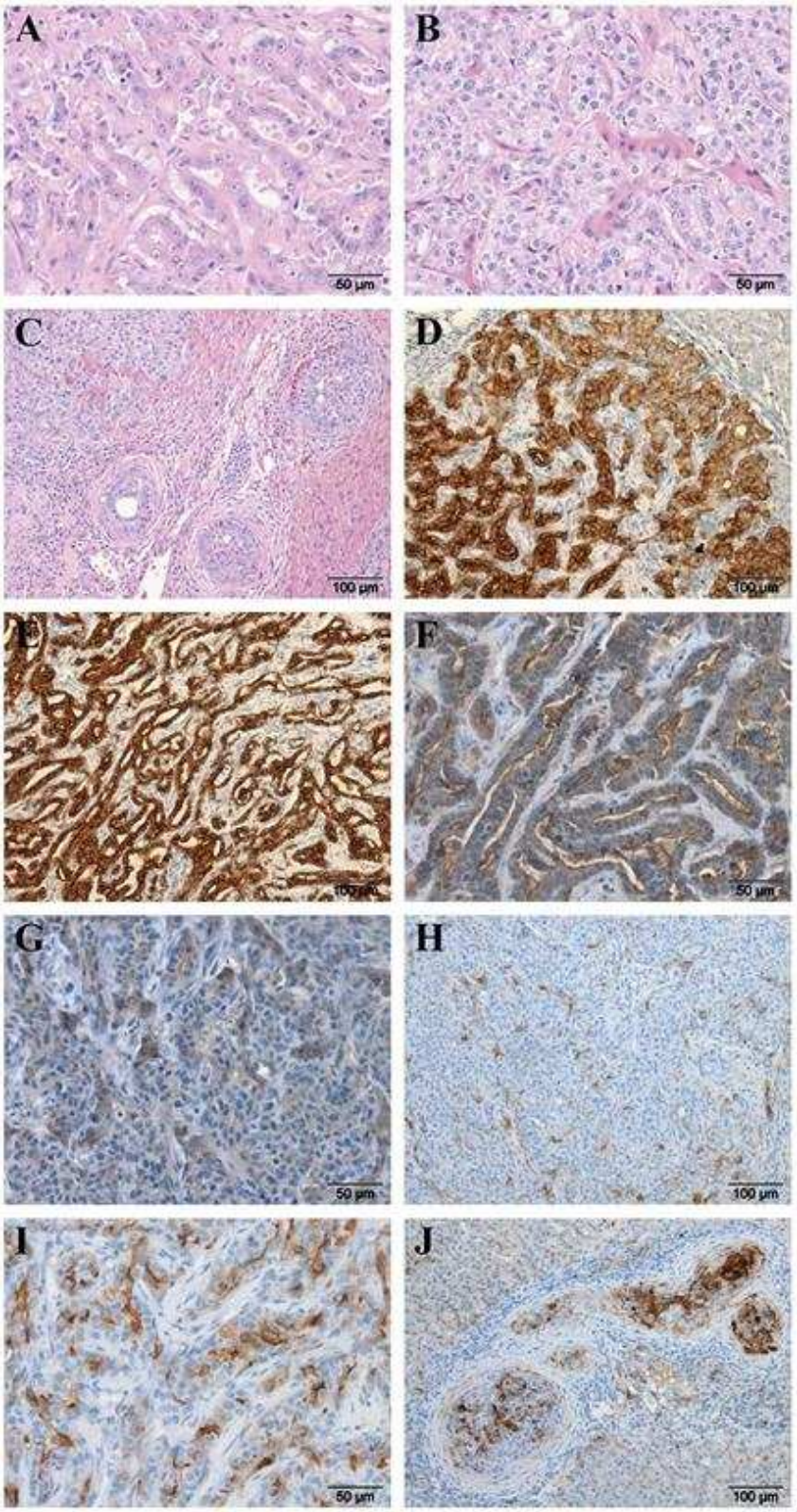

Fig. 8. Canine cholangiolocarcinoma. (A) HE, central tubular areas with fibrosis; (B) HE: peripheral solid area; (C) HE, vascular invasion; (D) K19, marked staining of central tubular (lower left) and less intense staining of peripheral solid areas (upper right); (E) K19, tubular areas with cytoplasmic and more pronounced membranous staining of tumour cells; (F) EMA/MUC-1, tubular areas with apical and some cytoplasmic staining; (G) EMA/MUC-1, negative staining of solid neoplastic areas, slight non-specific staining of pre-existent hepatic cords; (H) CD10, solid peripheral area with negative staining of neoplastic cells, some canalicular staining within pre-existent hepatic cords; (I) CD10, tubular areas with positive apical and some cytoplasmic staining; (J) CD10, moderate cytoplasmic staining of intravascular metastasis.

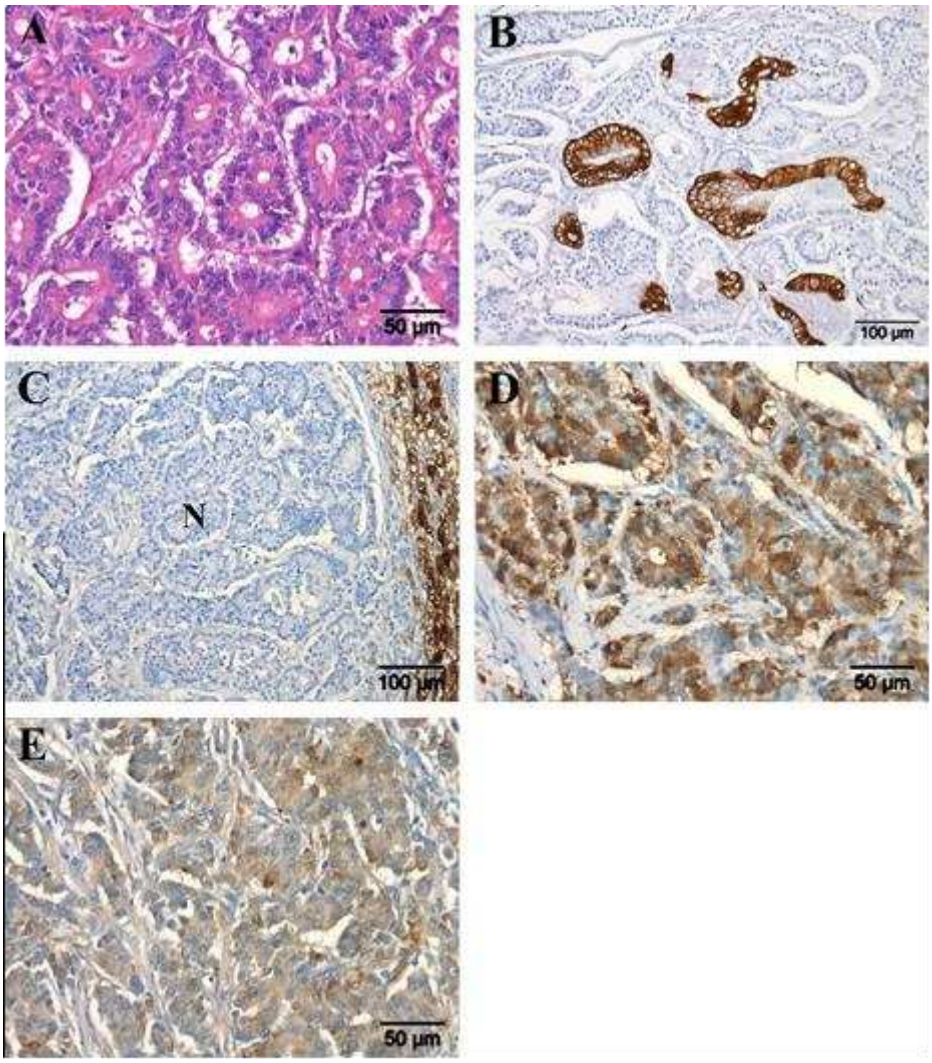

Fig. 9. Canine hepatic neuroendocrine carcinoma. (A) HE, rosette pattern with fine fibrovascular stroma; (B) K19, focal positive staining within tumour; (C) HepPar-1, negative staining of neoplastic tissue (N); (D) NSE, marked cytoplasmic staining of neoplastic cells; (E) CgA, moderate cytoplasmic staining of neoplastic cells

Table 4
Classification and immunohistochemical differentiation of the canine primary hepatic neoplasms.

	HepPar-1	K19	CD10	EMA/Muc-1	NSE	Cg-A
Nodular hyperplasia (n = 11)	+++	0	Canalicular + to +++	0	0	+/− (n = 2)
Hepatocellular adenoma (n = 62)	+++	0–5%	Canalicular + to +++	0	++ (n = 10)	+ (n = 1)
Hepatocellular carcinoma (n = 17)	0 (+)	+++	0	0	+ to ++ (n = 2)	+ (n = 1)
Scirrhous hepatocellular tumour (n = 3)	Ductular 0 trabecular +++	Ductular +++ trabecular 0	Ductular 0 trabecular + to ++	0	Ductular +++ trabecular 0	0
Cholangiocellular carcinoma (ductal type) (n = 3)	0	+++	0	+++	0	0
Cholangiocellular carcinoma (ductular type) (n = 6)	0	+++	+ to ++	+++	0 to ++ (n = 2)	0
Cholangiolocarcinoma (n = 1)	0	+++	Tubular ++ solid 0	Tubular ++ solid 0	0	+
Neuroendocrine carcinoma (n = 3)	0	0–5%	0	0	++ to +++	++

Cg-A, chromogranin-A; EMA/MUC-1, epithelial membrane antigen/mucin-1; K19, keratin 19; NSE, neuron-specific enolase.

There was a relatively low frequency (9%) of cholangiocellular tumours in our study, possibly because dogs have a low incidence of chronic biliary disease. Cholangiocellular neoplasms were associated with adult-type congenital cystic disease of the liver (van den Ingh et al., 2006) in 4/10 cases. All nine canine cholangiocellular carcinomas were positive for K19 and EMA/MUC-1 and were thought to be derived from differentiated mucin-producing cholangiocytes, normally present in larger bile ducts. Some of the tumours also showed CD10 positivity, which might suggest a ductular origin. All cholangiocellular tumours exhibited infiltrative growth, vascular invasion and intrahepatic and/or distant metastasis.

The cholangiolocarcinoma had a different morphology and immunohistochemical pattern in comparison with the cholangiocellular carcinomas, with tubular structures (K19, EMA/MUC-1 and CD10 positive) and solid hepatocyte-like areas (K19 positive and HepPar-1, EMA/MUC-1 and CD10 negative). This is suggestive of bidirectional differentiation of HPCs to hepatocytes and cholangiocytes (Komuta et al., 2008). No cholangiocellular adenomas were identified in our case series; these tumours are rare and it is likely that almost all of the cholangiocellular adenomas described in the veterinary literature represent adult-type cystic liver disease (Charles et al., 2006).

The primary hepatic neuroendocrine carcinomas identified in this study had a similar histological appearance to those described by Patnaik et al. (2005). These tumours are rare in the dog and most likely are derived from pre-existing neuroendocrine cells in the biliary epithelium. In this study the frequency of neuroendocrine carcinomas was low (3%) and all had intrahepatic metastases. All three tumours exhibited strong positive immunostaining for NSE, while positive staining for Cg-A was present in >30% cells in 2/3 tumours; they were negative or mostly negative for other markers.

Positive immunostaining for NSE was present in 10/62 well-differentiated hepatocellular tumours, 2/17 malignant hepatocellular tumours, ductular structures of 3/3 scirrhous hepatocellular tumours and 2/10 cholangiocellular carcinomas. Although this immunoreactivity might indicate neuroendocrine differentiation, it may be non-specific or could be driven by the stromal microenvironment, as might occur in scirrhous hepatocellular tumours. The positive staining for Cg-A in well differentiated malignant hepatocellular tumours, as well as in the cholangiolocarcinoma, more likely indicates that there is some neuroendocrine differentiation within these tumours, particularly since proliferating human HPCs express Cg-A (Roskams et al., 1990, 1991; Turner et al., 2011).

Conclusions

Histological and immunohistochemical examination of primary hepatic neoplasms in the dog can be used to differentiate various hepatocellular and cholangiocellular, as well as neuroendocrine, tumours. The proposed new classification in the dog is in accordance with the most recent classification scheme of primary hepatic neoplasms in humans. This standardised classification of the primary hepatic neoplasms in the dog could be used as a basis for assessment of therapeutic interventions.

Conflict of interest statement

None of the authors of this paper has a financial or personal relationship with other people or organisations that could inappropriately influence or bias the content of the paper.

Acknowledgements

We thank Lesley Anne de Groot and Kathleen van den Eynde for their technical support, and Valuepath for providing archival material.

References

Allison, M.R., Lovell, M., 2005. Liver cancer: The role of stem cells. Cell Proliferation 38, 407–421.

Al-Muhannadi, N., Ansari, N., Brahmi, U., Satir, A.A., 2011. Differential diagnosis of epithelial tumors in the liver: An immunohistochemical study on liver biopsy material. Annals of Hepatology 10, 508–515.

Boulter, L., Govaere, O., Bird, T.G., Radulescu, S., Ramachandran, P., Pellicoro, A., Ridgway, R.A., Soo Seo, S., Spee, B., Rooijen van, N., Sansom, O.J., Iredale, J.P., Lowell, S., Roskams, T., Forbes, S.J., 2012. Macrophage-derived Wnt opposes Notch signaling to specify hepatic progenitor cell fate in chronic liver disease. Nature Medicine 18, 572–579.

Charles, J.A., Cullen, J.M., van den Ingh, T.S.G.A.M., Van Winkle, T., Desmet, V.J., 2006. Morphological classification of neoplastic disorders of the canine and feline liver. In: Rothuizen, J. (Ed.), WSAVA Standards for Clinical and Histological Diagnosis of Canine and Feline Liver Diseases. Elsevier Health Sciences, Edinburgh, UK, pp. 117–124.

Cullen, J.M., Popp, J.A., 2002. Tumors of the liver and gall bladder. In: Meuten, D.J. (Ed.), Tumors in Domestic Animals, Fourth Ed. Iowa State University Press, Ames, Iowa, USA, pp. 483–504.

Desmet, V.J., 2011. Ductal plates in hepatic ductular reactions. Hypothesis and implications. 1. Types of ductular reaction reconsidered. Virchows Archiv 458, 251–259.

Durnez, A., Verslype, C., Nevens, F., Fevery, J., Aerts, R., Pirenne, J., Lesaffre, E., Libbrecht, L., Desmet, V., Roskams, T., 2006. The clinicopathological and prognostic relevance of Keratin 7 and 19 expression in hepatocellular carcinoma. A possible progenitor cell origin. Histopathology 49, 138–151.

Hammer, A.S., Sikkema, D.A., 1995. Hepatic neoplasia in the dog and cat. Veterinary Clinics of North America. Small Animal Practice 25, 419–435.

Komuta, M., Govaere, O., Vandecaveye, V., Akiba, J., Van Steenbergen, W., Verslype, C., Laleman, W., Pirenne, J., Aerts, R., Yano, H., Nevens, F., Topal, B., Roskams, T., 2012. Histological diversity in cholangiocellular carcinoma reflects the different cholangiocyte phenotypes. Hepatology 55, 1876–1888.

Komuta, M., Spee, B., Vander Borght, S., De Vos, R., Verslype, C., Aerts, R., Yano, H., Suzuki, T., Matsuda, M., Fujii, H., Desmet, V.J., Kojiro, M., Roskams, T., 2008. Clinicopathological study on cholangiolocellular carcinoma suggesting hepatic progenitor cell origin. Hepatology 47, 1544–1556.

Lamoureux, J.L., Carreira, V.S., Fitzgerald, S.D., Langohr, I.M., Rebecca, C., Smedley, R.C., 2012. Pathology in practice. Journal of the American Veterinary Medical Association 241, 1591–1593.

Lau, K.L., Prakash, S., Geller, S.A., Alsabeh, R., 2002. Comparative immunohistochemical profile of hepatocellular carcinoma, cholangiocarcinoma, and metastatic adenocarcinoma. Human Pathology 33, 1175–1181.

Libbrecht, L., Roskams, T., 2002. Hepatic progenitor cells in human liver diseases. Seminars in Cell and Developmental Biology 13, 389–396.

Libbrecht, L., 2006. Hepatic progenitor cells in human liver tumor development. World Journal of Gastroenterology 12, 6261–6265.

Morrison, C., Marsh Jr, W., Frankel, W.L., 2002. A comparison of CD10 to pCEA, MOC-31, and hepatocyte for the distinction of malignant tumors in the liver. Modern Pathology 15, 1279–1287.

Parkin, D.M., Bray, F., Ferlay, J., Pisani, P., 2001. Estimating the world cancer burden: Globocan 2000. International Journal of Cancer 94, 153–156.

Patnaik, A.K., Hurvitz, A.I., Lieberman, P.H., 1980. Canine hepatic neoplasms: A clinicopathologic study. Veterinary Pathology 17, 553–564.

Patnaik, A.K., Lieberman, P.H., Hurvitz, A.I., Johnson, G.F., 1981. Canine hepatic carcinoids. Veterinary Pathology 18, 445–453.

Patnaik, A.K., Newman, S.J., Scase, T., Erlandson, R.A., Antonescu, C., Craft, D.,

Bergman, P.J., 2005. Canine hepatic neuroendocrine carcinoma: An immunohistochemical and electron-microscopic study. Veterinary Pathology 42, 140–146.

Roskams, T., 2006. Different types of liver progenitor cells and their niches. Journal of Hepatology 45, 1–4.

Roskams, T., De Vos, R., van den Oord, J.J., Desmet, V., 1991. Cells with neuroendocrine features in regenerating human liver. APMIS Suppl. 23, 32–39. Roskams, T., van den Oord, J.J., De Vos, R., Desmet, V.J., 1990. Neuroendocrine features of reactive bile ductules in cholestatic liver disease. American Journal of Pathology 137, 1019–1025.

Seok, J.Y., Na, D.C., Woo, H.G., Roncalli, M., Kwon, S.M., Yoo, J.E., Ahn, E.Y., Kim, G.I., Choi, J.S., Kim, Y.B., Park, Y.N., 2012. A fibrous stromal component in hepatocellular carcinoma reveals a cholangiocarcinoma-like gene expression trait and epithelial–mesenchymal transition. Hepatology 55, 1776–1786.

Stalker, M.J., Hayes, M.A., 2007. Liver and biliary system. In: Maxie, G.M. (Ed.), Jubb, Kennedy, and Palmer's Pathology of Domestic Animals. Elsevier Health Sciences, Edinburgh, UK, pp. 382–387.

Turner, R., Lozoya, O., Wang, Y., Cardinale, V., Gaudio, E., Alpini, G., Mendel, G., Wauthier, E., Barbier, C., Alvaro, D., Reid, L.M., 2011. Human hepatic stem cell and maturational liver lineage biology. Hepatology 53, 1035–1045.

van den Ingh, T.S.G.A.M., Cullen, J.M., Twedt, D.C., van Winkle, T., Desmet, V.J., Rothuizen, J., 2006. Morphological classification of biliary disorders of the canine and feline liver. In: Rothuizen, J. (Ed.), WSAVA Standards for Clinical and Histological Diagnosis of Canine and Feline Liver Diseases. Elsevier Health Sciences, Edinburgh, UK, pp. 117–124.

van Sprundel, R.G., van den Ingh, T.S., Desmet, V.J., Katoonizadeh, A., Penning, L.C., Rothuizen, J., Roskams, T., Spee, B., 2010. Keratin 19 marks poor differentiation and a more aggressive behaviour in canine and human hepatocellular tumours. Comparative Hepatology 9, 4.

Wang, Y., Yao, H.L., Cui, C.B., Wauthier, E., Barbier, C., Costello, M.J., Moss, N., Yamauchi, M., Sricholpech, M., Gerber, D., Loboa, E.G., Reid, L.M., 2010. Paracrine signals from mesenchymal cell populations govern the expansion and differentiation of human hepatic stem cells to adult liver fates. Hepatology 52, 1443–1454.

Watson, P., 2005. Diseases of the liver. In: Hall, E.J., Simpson, J.W., Williams, D.A. (Eds.), BSAVA Manual of Canine and Feline Gastroenterology. British Small Animal Veterinary Association, Quedgeley, Gloucester, UK, pp. 264–266.

Yeh, M.M., 2010. Pathology of combined hepatocellular–cholangiocarcinoma. Journal of Gastroenterology and Hepatology 25, 1485–1492.